

Design of High-Channel-Count Multichannel Fiber Bragg Gratings Based on a Largely Chirped Structure

Yitang Dai and Jianping Yao, *Senior Member, IEEE*

Abstract—We propose a novel technique to design a high-channel-count, multichannel fiber Bragg grating (FBG) based on a largely chirped structure. The minimization of refractive-index modulation has been widely discussed in the previously demonstrated multichannel grating designs. The complexity of the grating structure, however, is also important from the point of view of practical fabrication. In this paper, the degree of grating complexity (DGC) is defined. We show that the DGC of a multichannel grating can be significantly reduced by designing a grating with a largely chirped structure. A detailed grating design process based on this technique is discussed, by which four multichannel gratings are designed and numerically studied, for applications such as periodic and nonperiodic spectral filtering, chromatic dispersion compensation and dispersion slope compensation. The proposed theory and examples show that different gratings with high-channel-count and multichannel responses can be designed and fabricated using a single commercially available phase mask, and all the gratings can be realized by a conventional FBG fabrication facility since the gratings have a low DGC with low index modulation.

Index Terms—Dispersion compensation, dispersion slope, fiber Bragg grating (FBG), multichannel.

I. INTRODUCTION

FIBER Bragg gratings (FBGs) have found important applications in optical communications, sensors, and other optical systems, thanks to the advantageous features such as small size, low loss, high reliability, and compatibility with other fiber components. An FBG with a multichannel spectral response is highly desirable in a wavelength-division-multiplexing (WDM) system, to perform functions such as multiwavelength filtering and multichannel chromatic dispersion management. Therefore, the design and realization of a multichannel high-channel-count FBG have been topics of interest recently.

Although many design approaches have been proposed [1], a high-channel-count multichannel FBG is very difficult to realize due to the requirement for both a high index modulation and a very complicated structure. The previously demonstrated approaches are usually trying to optimize the grating structure, to reduce the index modulation to a practically achievable

value. An FBG based on the conventional amplitude sampling technique has a simple structure, but the required index modulation is in proportion to the channel number N [2]. Buryak *et al.* in [3] provided a solution by modeling a multichannel grating as a superposition of many subgratings. They showed that, by dephasing the subgratings, the required index modulation will be proportional to \sqrt{N} , which is reduced significantly, making the fabrication of the multichannel FBG practically possible. For example, based on the phase-only sampling technology, multichannel FBGs for multichannel filtering and chromatic dispersion compensation have been proposed and experimentally demonstrated [4]–[6]. Another problem that limits the practical applications of multichannel FBGs is that a multichannel grating usually has a very complicated structure. For example, in the phase-only sampling technique, deep phase modulation is required. Therefore, a very fine-scale structure is required; the interval between two adjacent phase shifts is as small as $10\ \mu\text{m}$, to achieve a grating with a 100-GHz channel spacing and a channel number of 51 [7]. Such a grating cannot be fabricated with a conventional FBG fabrication system, unless a special phase mask is available. The realization of such a fine-scale phase mask is also complicated [5], with different gratings using different phase masks, making the grating fabrication inflexible and costly.

The spectral Talbot effect provides another way to realize high-channel-count multichannel gratings, which is based on an interference effect among the individual overlapped channels [8]–[11]. This technique has the flexibility and capability in achieving multichannel FBGs with various channel spacing and dispersions by using only one phase mask. The advantage of this technique is that the designed grating has a much simpler structure than that designed by the phase-only sampling technique, so that it can be fabricated by the conventional FBG fabrication technique. FBGs with a channel spacing of 100 GHz, and a channel count of 40 for multichannel filtering and chromatic dispersion compensation have been experimentally demonstrated [10], [11]. There are, however, two problems that have not yet been resolved. First, in addition to the desired in-band channels, there exist a large number of out-band channels which should be eliminated. Second, the spectral responses of the channels are identical or very similar. For many applications, however, the spectral responses of the channels should not be identical. For example, the filter used in an optical add-drop multiplexer (OADM) should have a nonperiodic frequency response. A multichannel dispersion compensator should have different dispersion values in different channels, which has to be achieved by slightly chirping the sampling period and will result in a nonflat reflection response and nonuniform channel bandwidth. Design

Manuscript received October 16, 2008; revised December 17, 2008. Current version published July 01, 2009. The work was supported by the Natural Sciences and Engineering Research Council of Canada (NSERC).

The authors are with the Microwave Photonics Research Laboratory, School of Information Technology and Engineering, University of Ottawa, Ottawa, ON, K1N 6N5, Canada (e-mail: jpyao@site.uottawa.ca).

Color versions of one or more of the figures in this paper are available online at <http://ieeexplore.ieee.org>.

Digital Object Identifier 10.1109/JQE.2009.2015585

techniques based on various multichannel grating reconstruction algorithms [12], [13] have been proposed to solve the problems. However, the gratings are still too complicated to be fabricated using the conventional FBG fabrication technique.

In this paper, we propose a novel approach to designing multichannel gratings based on a largely chirped structure. The problems discussed above can be eliminated by the proposed technique: a nonperiodic multichannel spectral response, or a spectral response with the channels having different properties, can be designed. Meanwhile, the out-band channels can be suppressed. The key advantage of the proposed approach is that the required index modulation is low, and the gratings can be fabricated by the conventional FBG fabrication technique, with different gratings fabricated based on a single commercially available phase mask.

The remainder of this paper is organized as follows. The principle of the proposed technique is described in Section II, which is proposed from the point of view of practical fabrication. A model to describe the conventional grating fabrication system is established, and the degree of grating complexity (DGC) is defined to describe the level of difficulty to fabricate a grating. Then, the DGCs of a regular multichannel grating and a grating based on the proposed design are theoretically analyzed, and we conclude that the DGC can be decreased greatly when designing a multichannel FBG with a largely chirped structure. In Section III, four design examples including a periodic and a nonperiodic filters, a chromatic dispersion compensator, and a dispersion slope compensator, are numerically studied. All these design are made based on a commercially available chirped phase mask. The DGCs are small and the index modulations are low, which enable the fabrication of the gratings using a conventional FBG fabrication facility. In Section IV, the required index modulation is discussed, and a conclusion is drawn.

II. PRINCIPLE

A. Degree of Grating Complexity

One difficulty in the fabrication of a multichannel FBG is the requirement for an ultralarge index modulation. Many approaches have been proposed recently to minimize the index modulation [3], [12], [13]. The problem existing in these approaches is that a multichannel FBG with an optimized design has a fine-scale and complicated structure when a high channel count is required, which can be hardly fabricated using a conventional FBG fabrication system.

To solve this problem, in this paper we proposed a novel technique to design a grating with a high channel count with a simple structure and low index modulation, which can be fabricated using a conventional FBG fabrication system. Before demonstrating the novel approach, we define a new parameter called degree of grating complexity (DGC). Mathematically, an FBG that is fabricated based on the phase mask technology using a UV light with side writing can be described by

$$\kappa(z) = \kappa_W(z) \exp \left[j \frac{2\pi}{\Lambda} z + j\varphi(z) \right] \quad (1)$$

where $\kappa(z)$ is the coupling coefficient of the grating, Λ is the mean grating period, and $\varphi(z)$ is the phase modulation which

is introduced by the phase mask. For example, for a grating that is based on a chirped phase mask, $\varphi(z)$ is given

$$\varphi(z) = -\frac{\pi C}{\Lambda^2} z^2 \quad (2)$$

where C is the chirp rate of the grating. $\kappa_W(z)$ (which is usually a complex function containing both amplitude and phase) is then the coupling coefficient profile which is actually implemented during the fabrication. Clearly, the DGC should be determined by $\kappa_W(z)$ rather than $\kappa(z)$, in terms of the grating fabrication. For example, to fabricate a grating for chromatic dispersion compensation, $\kappa_W(z)$ is just a super-Gaussian function without any phase modulation, if a proper chirped phase mask is used. An intuitive conclusion is that the DGC would be high if $\kappa_W(z)$ changes rapidly versus z along the grating.

To describe the DGC in quantity, a model for the fabrication platform is established. In many fabrication systems, especially those in the laboratories, the UV light is from a frequency-doubled argon-ion laser, with the beam focused so that the energy can be much higher at the focus point, especially for the fabrication of a grating with a complicated structure, the UV light with a fine UV beam should be used, as we will discuss below. Assuming that the UV-beam-induced coupling coefficient profile along the grating is normalized as $q(z)$, to form a long grating, such a UV exposure should be made in a series of positions along the fiber

$$\hat{\kappa}_W(z) = q(z) * \sum_{k=1}^M \alpha_k \delta(z - kP) \quad (3)$$

where M is the number of exposures, $\delta(t)$ is the unit impulse function, P is the interval between the adjacent exposure points, α_k is the coupling coefficient strength, which can be controlled by the exposure time, and $*$ denotes the convolution operation. To fabricate a complicated grating, phase shift should be introduced so that α_k is a complex number. Usually, such a phase modulation is not introduced by the phase mask; instead, it is introduced during the fabrication by a high-precision translation stage, such as a piezoelectric transducer (PZT). A commercially available PZT can have an effective resolution in the sub-nanometer range [14]; a precise phase modulation can therefore be achieved using such a PZT.

The fabrication process is actually to optimize α_k so that $\hat{\kappa}_W(z)$ can approach to the desired $\kappa_W(z)$

$$q(z) * \sum_{k=1}^M \alpha_k \delta(z - kP) \rightarrow \kappa_W(z). \quad (4)$$

Mathematically, this problem can be solved by taking the Fourier transform on both sides of (4) to yield

$$\sum_{k=1}^M \alpha_k \exp(-jkP \times 2\pi\sigma) \rightarrow \frac{K_W(2\pi\sigma)}{Q(2\pi\sigma)} \quad (5)$$

where $K_W(2\pi\sigma)$ and $Q(2\pi\sigma)$ are the Fourier transforms of $\kappa_W(z)$ and $q(z)$, respectively, and σ is the spatial frequency. From (5), we can see that the bandwidth of $K_W(2\pi\sigma)$, B_{KW} , is determined by two factors. First, B_{KW} should be less than B_Q , the bandwidth of $Q(2\pi\sigma)$, since $K_W(2\pi\sigma)$ is the sum of

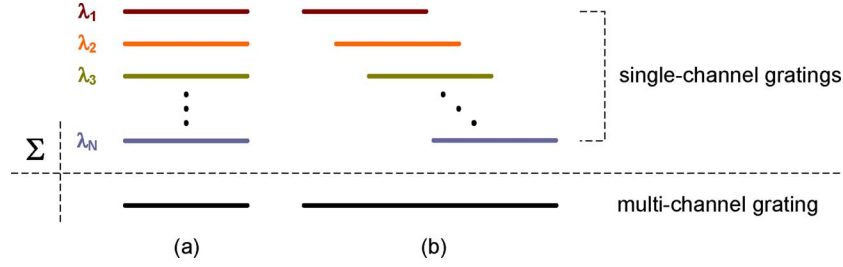


Fig. 1. Multichannel grating design based on (a) a uniform phase mask and (b) a chirped phase mask.

$Q(2\pi\sigma)$. Second, (5) shows that the left-hand-side equation is just the Fourier series expansion of the right-hand-side equation; however, based on the Fourier series expansion theory, the bandwidth of the right-hand side should be confined within $1/P$. As a result, to fabricate a grating with a large B_{KW} , a fine UV beam is required as well as a small exposure interval. A grating that can be fabricated should have a B_{KW} that is smaller than the maximum B_Q achievable by an FBG fabrication system. Since it is required that $B_{KW} < B_Q$, and the product of the length of $q(z)$, L_q (i.e., the width of the UV beam), and B_Q is about one, then we have

$$L_q < \frac{1}{B_{KW}}. \quad (6)$$

Equation (6) gives an upper limit of the width of the UV beam, that is, the finesse that the beam of the fabrication system should at least have. Then L_q can be defined as the DGC of the desired grating, which is a parameter that specifies the finesse of the fabrication system that can fulfill the fabrication task.

The DGC can be used to measure the level of difficulty in fabricating a multichannel grating. Many previously reported multichannel grating design techniques, such as the phase-only sampling technique and the techniques in [3], [12], [13], are based on the use of a chirp-free phase mask, that is, $\varphi(z) = 0$ in (1). If a weak grating is considered, the grating spectrum is then just the Fourier transform of $\kappa(z)$, which is precisely $K_W(4\pi\sigma)$ (note that $\varphi(z) = 0$ here). The relationship between σ and the light wavelength λ is

$$\sigma = \frac{n_{\text{eff}}}{\lambda} - \frac{1}{2\Lambda} \approx \frac{\Delta\lambda}{4n_{\text{eff}}\Lambda^2} \quad (7)$$

where n_{eff} is the effective refractive index of the fiber and $\Delta\lambda$ is the distance between the light wavelength and the Bragg wavelength of the FBG. Based on (6) and (7), we can see that, if the total bandwidth of the required multichannel grating is B_G , the grating DGC should be

$$\begin{aligned} B_{KW} &= \frac{B_G}{2n_{\text{eff}}\Lambda^2} \\ L_q &< \frac{\Lambda^2}{\frac{B_G}{2n_{\text{eff}}}} \end{aligned} \quad (8)$$

As an example, if an FBG has a channel number of 51 with a channel spacing of 100 GHz, the total bandwidth B_G would be about 40 nm, and then the beam width L_q should be less than

20 μm . Such a fine-scale UV exposure is hard to achieve in the core of a single-mode fiber since the standard single-mode fiber has a large radius of 62.5 μm . To fabricate an FBG with a high DGC, the fine-scale structures of the FBG are usually encoded in the phase mask, such as the phase-only sampling technique [4]–[7]. In terms of the DGC, the phase-only sampling moves the required phase modulation from $\kappa_W(z)$ to $\varphi(z)$, by which the DGC is decreased greatly: $\kappa_W(z)$ for a multichannel grating is then the same as that for a single-channel grating.

In brief, any multichannel grating with $\varphi(z) = 0$ has a high DGC and cannot be fabricated by the conventional FBG fabrication technique. In this paper, the design of a multichannel FBG with a largely chirped structure to ease the fabrication difficulty is proposed, where the value of the DGC is significantly decreased. Compared with the phase-only sampling technique, a multichannel FBG designed based on the proposed technique can be fabricated with a conventional FBG fabrication system using a commercially available phase mask.

B. Design of a Multichannel Grating With a Largely Chirped Structure

Fig. 1 shows the difference between the conventional multichannel grating design and the proposed technique which is based on a largely chirped structure. Generally, a multichannel grating can be designed by summing multiple single-channel gratings

$$\begin{aligned} \kappa(z) &= \sum_{l=1}^N \kappa_l(z) \exp\left(j\frac{2\pi}{\Lambda_l}z\right) \\ &\approx \sum_{l=1}^N \kappa_l(z) \exp\left(-j\frac{2\pi\Delta\Lambda_l}{\Lambda^2}z\right) \times \exp\left(j\frac{2\pi}{\Lambda}z\right) \end{aligned} \quad (9)$$

where $\kappa_l(z)$ and Λ_l are the coupling coefficient profile and period of the l th grating, respectively, Λ is the mean grating period, and $\Delta\Lambda_l = \Lambda_l - \Lambda$. In the conventional summing schemes, such as the phase-only sampling, all the subgratings are superimposed at the *same* position, as shown in Fig. 1(a), which results in a high DGC. In the proposed grating design, however, the subgratings are located at different positions

$$\kappa(z) = \sum_{l=1}^N \kappa_l(z - z_l) \exp\left(-j\frac{2\pi\Delta\Lambda_l}{\Lambda^2}z\right) \times \exp\left(j\frac{2\pi}{\Lambda}z\right). \quad (10)$$

In our design, such a grating is fabricated based on a chirped phase mask with a chirp rate of C . Therefore, based on (1), (2), and (10), we have

$$\kappa_W(z) = \sum_{l=1}^N \kappa_l(z - z_l) \exp\left(-j\frac{2\pi\Delta\Lambda_l}{\Lambda^2}z + j\frac{\pi C}{\Lambda^2}z^2\right) \quad (11)$$

which is what we should actually fabricate, and the DGC of the novel multichannel grating is then determined by (11). We take the l th subgrating as the following example:

$$\begin{aligned} \kappa_{W,l}(z) &= \kappa_l(z - z_l) \exp\left(-j\frac{2\pi\Delta\Lambda_l}{\Lambda^2}z + j\frac{\pi C}{\Lambda^2}z^2\right) \\ &= \kappa_l(x) \exp\left(j\frac{\pi C}{\Lambda^2}x^2 + j\beta_l x + j\theta_l\right) \end{aligned} \quad (12)$$

where $x = z - z_l$ and

$$\begin{aligned} \beta &= \frac{2\pi}{\Lambda^2}(Cz_l - \Delta\Lambda_l) \\ \theta_l &= \frac{\pi}{\Lambda^2}(Cz_l^2 - 2\Delta\Lambda_l z_l). \end{aligned} \quad (13)$$

In our design, we select the grating structure parameters such that $\beta_l \equiv 0$ for each l , then

$$z_l = \frac{\Delta\Lambda_l}{C}. \quad (14)$$

The bandwidth of $\kappa_{W,l}(z)$ can be calculated by taking the Fourier transform of (12) to get $K_{W,l}(2\pi\sigma)$. To simplify the analysis, we assume that $\kappa_l(x)$ is a Gaussian function with a full-width at half-maximum (FWHM) of $L_{s,l}$, which is an approximation of the length of the subgrating in a real case. Then, by the Fourier transform, the bandwidth of $K_{W,l}(2\pi\sigma)$ is

$$B_{KW,l} = \frac{L_{s,l}}{\pi} \sqrt{\left(\frac{4 \ln 2}{L_{s,l}^2}\right)^2 + \left(\frac{\pi C}{\Lambda^2}\right)^2} \quad (15)$$

which could be further simplified when the following conditions are considered. First, from (14), one can see that the whole grating length should be in inverse proportion to the chirp rate. In order to limit the grating length in an acceptable range (e.g., about 10 cm), the chirp rate should be large. Second, the lengths of the subgratings are usually in the order of several centimeters. Then, in (15), the right term is much larger than the left term under the radical sign. Therefore

$$B_{KW,l} = \frac{L_{s,l}C}{\Lambda^2}. \quad (16)$$

It should be noted that, once (14) is satisfied, the center spatial frequency of $K_{W,l}(2\pi\sigma)$ is located at $\sigma = 0$ for each subgrating, because $\beta_l = 0$ in (12). Since the multichannel grating is the sum of N such subgratings, the DGC B_{KW} is then the bandwidth that all the subgratings will cover. Obviously, B_{KW} is the maximum of $B_{KW,l}$. Assuming that L_s is the maximum among $L_{s,l}$, then we get

$$\begin{aligned} B_{KW} &= \frac{L_s C}{\Lambda^2} \\ L_q &< \frac{\Lambda^2}{L_s C}. \end{aligned} \quad (17)$$

Comparing with (8), one can see that the required finesse of the system will be decreased by choosing a proper C as

$$\frac{L_q}{L_q^0} = \frac{B_G}{2n_{\text{eff}}CL_s} \quad (18)$$

where L_q^0 is the required finesse for the original design ($\varphi(z) = 0$). In addition, the grating length is also changed. From Fig. 1(a), we can see that, in the original design, the grating length is actually L_s ; however, in the proposed design in Fig. 1(b), the grating length should be L_s plus the displacement of the subgratings, which is $B_G/2n_{\text{eff}}C$ from (14). Then, the grating length change can be expressed as

$$\frac{L}{L^0} = 1 + \frac{B_G}{2n_{\text{eff}}CL_s} = 1 + \frac{L_q}{L_q^0} \quad (19)$$

where L and L^0 are the lengths for the proposed grating and the original design, respectively.

From (18) and (19), one can see the advantage of a multichannel grating design based on a largely chirped structure: with the chirped structure, the DGC can be decreased by increasing the grating length. For example, for the grating with 100-GHz channel spacing and 51 channels, if we assume L_s is 4 cm and C is 1.2 nm/cm, then L_q is about 60 μm , which is about three times the beam width in the original design and can be realized by a conventional FBG fabrication system. However, the grating length is increased to about 16 cm. Currently, largely chirped phase masks having a length of up to 14 cm (e.g., phase masks from StockerYale, Inc) are commercially available. A long chirped grating fabricated by a long chirped mask has been recently reported [11]. It can be seen that the proposed technique to design a multichannel grating based on a largely chirped structure is especially suitable for a grating with a spectral response corresponding to a small L_s .

Another advantage of the proposed design is that the subgrating, i.e., the spectral responses of the channels, are not limited to be identical for all the channels, and the channel spacing is not required to be uniform either. This is different from the conventional grating design techniques, such as the technique based on sampling, where the spectral responses of the channels and the channel spacing should always be identical. Therefore, the proposed technique shows great flexibility for grating design and fabrication. To demonstrate the effectiveness of the proposed technique, a few design examples are provided in Section III.

III. SIMULATION EXAMPLES

To design a grating based on the proposed technique, one should perform the following steps.

Step 1) Define the grating coupling coefficient.

The grating structure can be designed directly based on (9), with each subgrating being defined separately. A better way is to calculate $\kappa(z)$ by a reconstruction algorithm from the desired multichannel frequency response

$$H(\omega) = \sum_{l=1}^N H_l(\omega - \omega_l) \times \exp(-j\omega\tau_l) \quad (20)$$

where $H(\omega - \omega_l)$ is the desired response in the l th channel, which is a complex function with both the amplitude and the phase responses, ω_l is the center angular frequency of the l th channel, and τ_l is the time delay of the l th channel, which is different for different channels because the subgratings are superimposed at different locations, as defined in (14). Then

$$\tau_l = \frac{2n_{\text{eff}}z_l}{c} = \frac{\lambda_l - \bar{\lambda}}{c \times C} \quad (21)$$

where c is the light speed in vacuum, λ_l is the center wavelength of the l th channel, and $\bar{\lambda}$ is the mean wavelength of all of the channels. By using an FBG reconstruction algorithm, such as the discrete layer peeling (DLP) method [15], the coupling coefficient of the whole grating, $\kappa(z)$, can then be achieved.

Step 2) Calculate the coupling coefficient profile.

The coupling coefficient profile defines the FBG that should be actually fabricated. Since the grating is fabricated by a chirped phase mask, the desired coupling coefficient profile, $\kappa_W(z)$, is then obtained based on (2) to yield

$$\kappa_W(z) = \kappa(z) \exp\left(j\frac{\pi C}{\Lambda^2} z^2\right). \quad (22)$$

Step 3) Select the proper $q(z)$ and P .

As discussed in Section II-A, $1/P$ and the bandwidth of $Q(2\pi\sigma)$ should be larger than the bandwidth of $K_W(2\pi\sigma)$.

Step 4) Calculate α_k .

Finally, the coupling coefficient strength and the phase at each UV exposure position can be obtained from (5). As discussed earlier, α_k is the Fourier series expansion coefficients of $K_W(2\pi\sigma)/Q(2\pi\sigma)$. It should be noted that the considered bandwidth should be confined within $|\sigma| \leq 1/2P$.

Based on the above design process, four examples are numerically studied in this section, to show the capacity of the proposed multichannel grating design technique. In the examples, the desired spectral responses are defined by following parameters: the channel number N is 51 and channel spacing is 100 GHz; in each single channel, the reflection spectrum has a fourth-order super-Gaussian profile with a reflectivity of 90% and a 3-dB bandwidth of 50 GHz. In the first step of each example, the desired frequency response is defined based on (20), and the coupling coefficient is calculated based on the DLP algorithm. To realize such gratings, the chirp rate C is -2.0 nm/cm, which means that the four gratings are designed and fabricated based on the same commercially available phase mask. The UV beam is assumed to have a Gaussian profile, which is a good approximation for many practical fabrication systems.

A. Ideal Multichannel Filtering

To perform multichannel filtering, the grating should be free of chromatic dispersion in each channel. Based on the design process, the coupling coefficient strength and the phase at each UV exposure position are calculated, which are shown in Fig. 2.

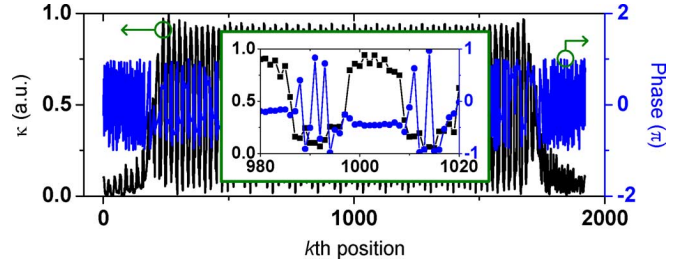


Fig. 2. Coupling coefficient strength and phase, α_k , at each UV exposure position. The insert shows the details of α_k at the center of the grating.

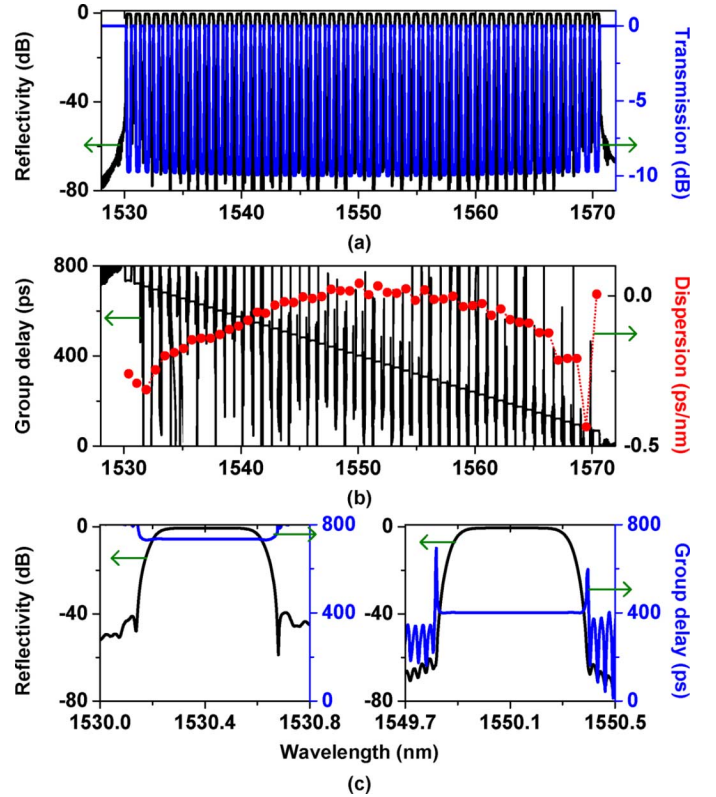


Fig. 3. Reflection spectrum of the grating with its design shown in Fig. 2. (a) The reflectivity and transmission spectra. (b) The group delay and dispersion. (c) The zoom-in spectra of the channels at the left edge and at the center.

One can see that the channels have an identical reflectivity of 90%, a 3-dB bandwidth of 0.4 nm, and zero dispersion, which are identical to the desired values. Fig. 3(c) shows the reflection and group delay responses of the 1st and the center channels, with identical channel performance demonstrated. A constant group delay difference between the two channels is observed, which is generated due to the largely chirped structure.

It should be noted that in the proposed multichannel grating the out-of-band reflectivity is significantly suppressed, leading to a diffraction efficiency of 100%, as shown in Fig. 3(a). This is very different from the gratings designed based on the Talbot effect or the phase-only sampling technique where the diffraction efficiency is always smaller than 100%. The reason of the excellent out-of-band reflectivity suppression is due to the fact that the grating structure is reconstructed directly from the desired frequency response, but not based on the sampling technique in

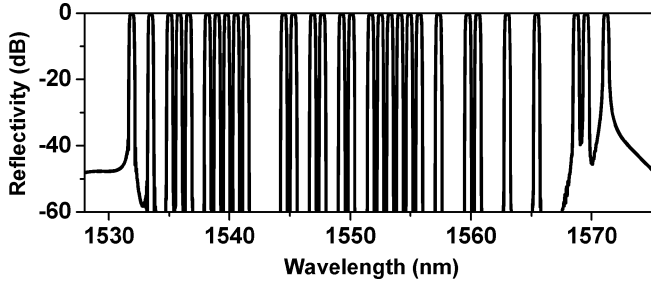


Fig. 4. Reflection spectrum of the grating with nonuniform channel spacing.

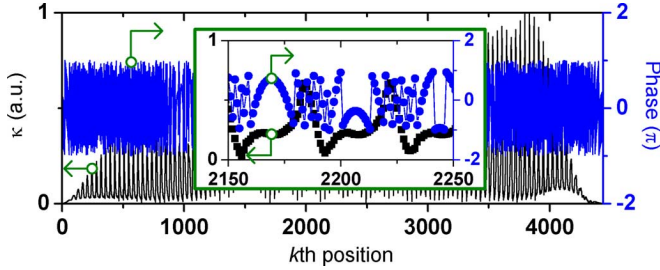


Fig. 5. Coupling coefficient strength and phase, α_k , at each UV exposure position. The insert shows the details of α_k at the center of the grating.

which the diffraction efficiency is hard to reach 100% [1]. Furthermore, the proposed technique can also be used to design a multichannel grating with nonperiodic channel spacing. Fig. 4 shows the spectral response of a multichannel grating having 51 channels with the reflectivities of either 90% or zero.

In the design of this nonuniformly spaced multichannel grating, the beam width L_q is still 0.12 mm, P is 0.046 mm, and the number of UV exposure points is 1703. The grating length is about 78 mm. The maximum index modulation used in our simulation is 6.9×10^{-4} .

B. Dispersion and Dispersion Slope Compensation

One of the important applications of a multichannel grating is dispersion compensation in an optical communication system. In our design, a multichannel grating with a dispersion of -660 ps/nm at 1550 nm and a dispersion slope of -2.4 ps/nm², corresponding to the chromatic dispersion of a length of 40 km single-mode fiber (dispersion parameter of 16.5 ps/nm/km at 1550 nm and a dispersion slope of 0.06 ps/nm²/km). Based on the proposed grating design process, the grating is designed with the distribution of α_k shown in Fig. 5.

Although the grating design, as shown in Fig. 5, is complicated, it can be fabricated by a conventional FBG fabrication system, since, in the design, the FWHM of the UV beam L_q is 0.06 mm, and exposure position interval P is 0.027 mm, which are practically implementable. The number of exposure points is 4438, and then the grating length is 120 mm. The maximum coupling coefficient is 1335 m^{-1} , corresponding to an index modulation of 6.6×10^{-4} .

The grating is designed and the reflection spectrum is shown in Fig. 6. As can be seen, the channels have an identical reflectivity of 90% and a 3-dB bandwidth of 0.4 nm. The dispersion

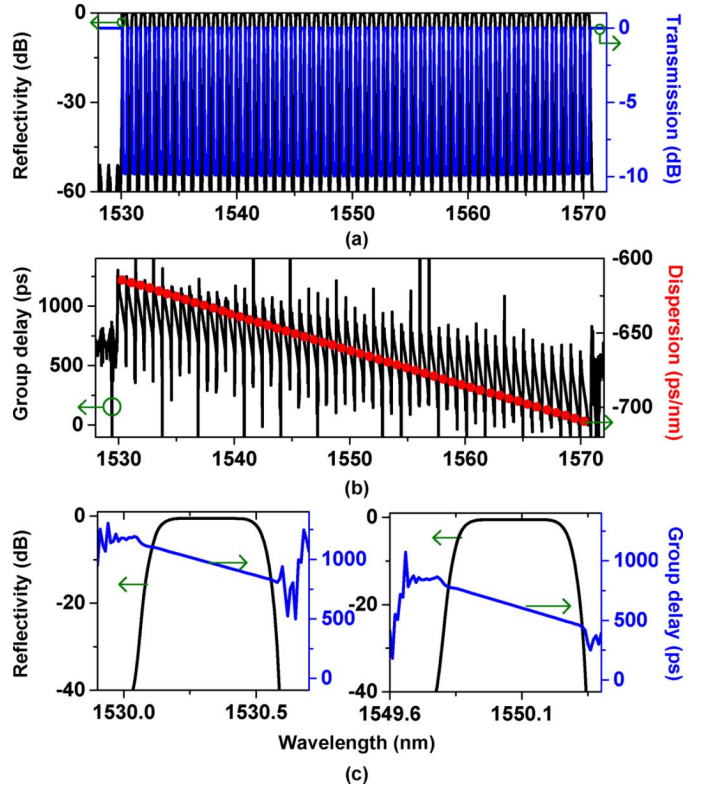


Fig. 6. Reflection spectrum of the grating with its design shown in Fig. 5. (a) The reflectivity and transmission spectra. (b) The group delay and dispersion. (c) The zoom-in spectra of the channels at the left edge and at the center.

varies from -614 to -709 ps/nm, and the dispersion slope is about 2.4 ps/nm².

In general, the length of a grating for dispersion compensation is proportional to the desired bandwidth and the dispersion. In our design, the length for each subgrating is about 2.7 cm. However, the total grating length is 12 cm, which is about four times the length of the subgrating. As can be seen, the DGC is decreased by increasing the length of the grating. If a larger dispersion in each channel is desired, the grating length will be longer than 12 cm, which requires a longer chirped phase mask. A grating with a short length is desirable for most of the applications. To realize a large dispersion in each channel (which is used in long-haul optical fiber transmission systems) by a single grating designed based on the proposed technique is difficult, which is the main limitation of this technique. However, multichannel dispersion gratings based on the proposed technique has other important applications [16], such as optical spectral filtering and not-long-haul dispersion compensation, where a grating with not-so-large dispersion value is required.

Another issue that should be addressed is the uniformity of the reflectivity among channels. In a sampling-based multichannel grating, the dispersion slope is achieved by slightly chirping the sampling period, which would result in the channel nonuniformity, that is, the reflectivity among channels will not be flat, and the bandwidths of the channels will not be identical either. In a grating designed based on our proposed technique, however, the uniformity is maintained throughout the channels. In the proposed technique, the grating structure is reconstructed directly from the desired spectral response, the

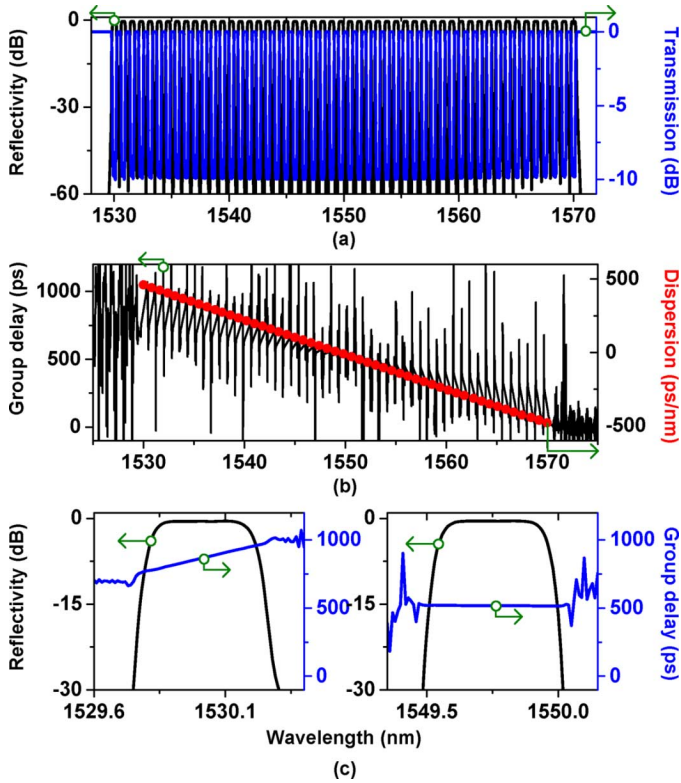


Fig. 7. Reflection spectrum of the grating designed for dispersion slope compensation. (a) The reflectivity and transmission spectra. (b) The group delay and dispersion. (c) The zoom-in spectra of the channels at the left edge and at the center.

dispersion slope will not show impact on the reflectivity profile, and the channel spectral responses are identical, as shown in Fig. 6(a) and (c). To demonstrate this property more clearly, a grating for multichannel dispersion slope compensation is designed. In this grating, the dispersion slope is 24 ps/nm^2 and the dispersion at the center channel is zero. Therefore, the grating can be used to compensate for the dispersion slope of about 400 km of single-mode fiber.

In the design of the grating, L_q is 0.80 mm, P is 0.043 mm, and the number of UV exposure points is 2770, so the grating length is about 120 mm. The maximum index modulation used in our simulation is 7×10^{-4} . The reflection spectrum is shown in Fig. 7.

It can be seen that the dispersion in each channel changes linearly from about -470 to 470 ps/nm within a bandwidth of 40 nm, which corresponds to a dispersion slope of 23.5 ps/nm^2 . The reflectivity profile of all the channels is kept unchanged, which is different from a multichannel grating designed based on the sampling technique with no-flat reflectivity profile.

IV. DISCUSSION AND CONCLUSION

In Section II, we have introduced the concept of DGC and have emphasized that DGC is an important factor that characterizes the difficulty and complexity in designing a multichannel grating. It is known, however, the index modulation is another factor that limits the number of channels of a multichannel grating. For the previously demonstrated multichannel

grating designs [2]–[8], the index modulation is between $\sqrt{N} \times \Delta n_s$ and $N \times \Delta n_s$, depending on the degree of dephase of the subgratings, where Δn_s is the index modulation of one of the subgratings. In the proposed technique, however, the N subgratings are not superimposed at the same position. Because of the largely chirped structure, there are only \tilde{N} subgratings written at the same positions, as shown in Fig. 1(b). To calculate \tilde{N} , we assume that the multichannel grating response is equally spaced. Based on (14), the distance between any two adjacent subgratings is $\Delta\lambda/2n_{\text{eff}}C$, where $\Delta\lambda$ is the channel spacing. Then, we have

$$\tilde{N} = \frac{2n_{\text{eff}}CL_s}{\Delta\lambda}. \quad (23)$$

Note that $B_G = N \times \Delta\lambda$; then, based on (18), we have

$$\frac{\tilde{N}}{N} = \frac{2n_{\text{eff}}CL_s}{B_G} = \frac{L_q}{L_q^0} \quad (24)$$

which means the required index modulation will also be decreased when L_q is increased, since the number of the superimposed subgratings is decreased. In the examples given in Section III, we assume that all of the subgratings are superimposed in-phase. The required index modulation is easy to be achieved. If an optimization algorithm is used to make the subgratings dephase, less index modulation is then required, and the required index modulation will be between $\sqrt{\tilde{N}} \times \Delta n_s$ and $\tilde{N} \times \Delta n_s$.

As a conclusion, we have proposed a novel approach to designing a multichannel grating based on a largely chirped structure. We have defined a new measure, called DGC, to characterize the difficulty in realizing a multichannel grating, which is associated with the beam finesse of the FBG fabrication system. We have shown that the DGC of a multichannel grating designed based on the previous techniques is too high to be fabricated by a conventional FBG fabrication system. In our proposed design, the DGC of a multichannel grating is reduced significantly thanks to the use of a largely chirped structure, as can be seen from (18). In addition, if the length of a grating is increased, the index modulation is decreased, which also simplifies the fabrication. Four gratings having 51 channels with a channel spacing of 100 GHz were designed and numerically evaluated. The advantages of the proposed technique: 1) different multichannel gratings can be fabricated using a single commercially available chirped phase mask; 2) no out-of-band channels are generated; 3) multichannel response with nonidentical subchannel responses and nonidentical channel spacing can be achieved; and 4) the multichannel gratings can be fabricated by a conventional FBG fabrication system that has a practically achievable beam finesse and low index modulation.

REFERENCES

- [1] H. Li, M. Li, Y. Sheng, and J. E. Rothenberg, "Advances in the design and fabrication of high-channel-count fiber Bragg gratings," *J. Lightw. Technol.*, vol. 25, no. 9, pp. 2739–2750, Sep. 2007.
- [2] M. Ibsen, M. K. Durkin, M. J. Cole, and R. I. Laming, "Sinc-sampled fiber Bragg gratings for identical multiple wavelength operation," *IEEE Photon. Technol. Lett.*, vol. 10, no. 6, pp. 842–844, Jun. 1998.
- [3] A. V. Buryak, K. Y. Kolossovski, and D. Y. Stepanov, "Optimization of refractive index sampling for multichannel fiber Bragg gratings," *IEEE J. Quantum Electron.*, vol. 39, no. 1, pp. 91–98, Jan. 2003.

- [4] J. E. Rothenberg, H. Li, Y. Li, J. Popelek, Y. Wang, R. B. Wilcox, and J. Zweiback, "Dammann fiber Bragg gratings and phase-only sampling for high channel counts," *IEEE Photon. Technol. Lett.*, vol. 14, no. 9, pp. 1309–1311, Sep. 2002.
- [5] J. E. Rothenberg, H. Li, Y. Sheng, J. Popelek, and J. Zweiback, "Phase only sampled 45 channel fiber Bragg grating written with a diffraction compensated phase mask," *Opt. Lett.*, vol. 31, no. 9, pp. 1199–1201, May 2006.
- [6] H. Li, M. Li, K. Ogusu, Y. Sheng, and J. E. Rothenberg, "Optimization of a continuous phase-only sampling for high channel-count fiber Bragg gratings," *Opt. Exp.*, vol. 14, no. 8, pp. 3152–3160, Apr. 2006.
- [7] J. Rothenberg, F. Babian, Z. Brodzeli, P. Chou, H. Li, Y. Li, J. Popelek, and R. Wilcox, "Phase-only sampling for fabrication and design of high channel-count fiber Bragg gratings," in *Proc. OFC*, 2003, ThL3.
- [8] C. Wang, J. Azana, and L. R. Chen, "Spectral Talbot-like phenomena in one-dimensional photonic bandgap structures," *Opt. Lett.*, vol. 29, no. 14, pp. 1590–1592, Jul. 2004.
- [9] X. Chen, J. Mao, X. Li, Z. Lin, S. Xie, and C. Fan, "High-channel-count comb fiber with a simple structure," in *Proc. OFC*, 2004, TuD2.
- [10] Y. Dai, X. Chen, X. Xu, C. Fan, and S. Xie, "High channel-count comb filter based on chirped sampled fiber Bragg grating and phase shifts," *IEEE Photon. Technol. Lett.*, vol. 17, no. 5, pp. 1040–1042, May 2004.
- [11] Y. Dai, X. Chen, J. Sun, and S. Xie, "Wideband multichannel dispersion compensation based on a strongly chirped sampled Bragg grating and phase shifts," *Opt. Lett.*, vol. 31, no. 3, pp. 311–313, Feb. 2006.
- [12] H. Li, T. Kumagai, K. Ogusu, and Y. Sheng, "Advanced design of a multichannel fiber Bragg grating based on a layer-peeling method," *J. Opt. Soc. Amer. B*, vol. 24, no. 11, pp. 1929–1938, Nov. 2004.
- [13] Q. Wu, P. L. Chu, and H. P. Chan, "General design approach to multichannel fiber Bragg grating," *J. Lightw. Technol.*, vol. 24, no. 3, pp. 1571–1580, Mar. 2006.
- [14] [Online]. Available: <http://www.physikinstrumente.com/en/products/prdetail.php?sortnr=200500>
- [15] R. Feced, M. N. Zervas, and M. A. Muriel, "An efficient inverse scattering algorithm for the design of nonuniform fiber Bragg gratings," *IEEE J. Quantum. Electron.*, vol. 35, no. 8, pp. 1105–1115, Aug. 1999.
- [16] Y. Dai and J. Yao, "Optical generation of binary phase-coded direct-sequence UWB signals using a multi-channel chirped fiber Bragg grating," *J. Lightw. Technol.*, vol. 26, no. 16, pp. 2513–2520, Aug. 2008.



Yitang Dai received the B.Sc. and Ph.D. degrees in electronic engineering from Tsinghua University, Beijing, China, in 2002 and 2006, respectively.

Since June 2007, he has been a Postdoctoral Research Fellow with the Microwave Photonics Research Laboratory, School of Information Technology and Engineering, University of Ottawa, Ottawa, ON, Canada. His research interests include fiber Bragg grating, optical CDMA, fiber lasers, microwave photonics, pulse shaping, semiconductor lasers, and optical sensors.



Jianping Yao (M'99–SM'01) received the Ph.D. degree in electrical engineering from the Université de Toulon, Toulon, France, in 1997.

He joined the School of Information Technology and Engineering, University of Ottawa, Ottawa, ON, Canada, in 2001, where he is currently a Professor, Director of the Microwave Photonics Research Laboratory, and Director of the Ottawa-Carleton Institute for Electrical and Computer Engineering. From 1999 to 2001, he held a faculty position with the School of Electrical and Electronic Engineering,

Nanyang Technological University, Singapore. He holds a guest Yongqian Endowed Chair Professorship with Zhejiang University, China. He spent three months as an Invited Professor with the Institut National Polytechnique de Grenoble, France, in 2005. His research has focused on microwave photonics, which includes all-optical microwave signal processing, photonic generation of microwave, mm-wave and THz, radio over fiber, UWB over fiber, fiber Bragg gratings for microwave photonics applications, and optically controlled phased-array antennas. His research interests also include fiber lasers, fiber-optic sensors, and bio-photonics. He is an Associate Editor of the *International Journal of Microwave and Optical Technology*. He has authored or coauthored over 120 papers in refereed journals and over 100 papers in conference proceeding.

Dr. Yao is a member of SPIE, the Optical Society of America and a senior member of the IEEE Photonics (formerly LEOS) and Microwave Theory and Techniques Societies. He is a Registered Professional Engineer of Ontario. He is on the Editorial Board of the *IEEE TRANSACTIONS ON MICROWAVE THEORY AND TECHNIQUES*. He was the recipient of the 2005 International Creative Research Award of the University of Ottawa and the 2007 George S. Glinski Award for Excellence in Research. He was named University Research Chair in Microwave Photonics in 2007, and he was a recipient of an NSERC Discovery Accelerator Supplements award in 2008.